Full Articles

Semiempirical method of calculations of transition-state geometries for radical addition reactions

A. F. Shestakov, E. T. Denisov, and N. S. Emel´yanova*

Institute of Problems of Chemical Physics, Russian Academy of Sciences, 142432 Chernogolovka, Moscow Region, Russian Federation. Fax: +7 (096) 515 5420. E-mail: edenisov@icp.ac.ru

Transition-state geometries of the addition reactions of $H^{\bullet}$, $^{\bullet}CH_3$, $^{\bullet}NH_2$, and $^{\bullet}OCH_3$ radicals to ethylene; $H^{\bullet}$ radical to acetylene, methyleneimine, acetonitrile, and formaldehyde; and $^{\bullet}CH_3$ radical to acetone and acetylene were determined by the density functional (B3LYP) method. The interatomic distances in the transition states of these reactions were also calculated from experimental data (enthalpies and activation energies) using the model of intersecting parabolas, the model of reduced intersecting parabolas (RIP), and the model of reduced intersecting parabola and Morse curve. The results obtained by different methods were compared and analyzed. An algorithm was elaborated for calculations of interatomic distances using experimental data, based on introduction of corrections to the RIP model.

Key words: aminyl radical, hydrogen atom, acetylene, acetonitrile, acetone, transition-state geometry, methyl radical, methoxyl radical, methyleneimine, method of intersecting parabolas, density functional theory, radical addition, method of reduced intersecting parabolas, method of reduced intersecting parabola and Morse curve, activation energy, enthalpy of reaction, ethylene.

Comparison of the interatomic distances in the transition states of radical abstraction reactions calculated using the model of intersecting parabolas (IP model) and by quantum chemistry methods led to elaboration of a simple algorithm of calculations of these parameters from experimental data (activation energies, E, and enthalpies of reactions, ΔH).[1—6] The algorithm is based on the introduction of a numerical coefficient (correction), β, close to unity in order to recalculate the total bond elongation, r_e, in the transition state ($r_e = \beta r_e$ (IP model)). This work is devoted to elaboration of a similar method for the determination of transition-state geometries of radical addition reactions.

Theoretical analysis of the quadratic dependence of the activation energy on the enthalpy of reaction (Polanyi—Semenov generalized relationship)

$$E = E_0 + \alpha\Delta H - \Delta H^2/(2W) \qquad (1)$$

shows that information on the transition-state structure can be extracted from the coefficient $W \approx |k^{\#}|r_e^2$, where

Published in Russian in *Izvestiya Akademii Nauk. Seriya Khimicheskaya,* No. 4, pp. 886—893, April, 2005.

1066-5285/05/5404-0905

$k^{\#}$ is the force constant of transition-state vibrational reaction mode characterized by an imaginary frequency. Consideration of radical abstraction reactions in the framework of the IP model gives an analogous interrelation between E and ΔH except that the coefficients at E_0 and W are related as follows

$$W = 8E_0 = k^* r_e^2 \qquad (2)$$

being determined by the force constant, k^*, of the C—H stretching vibration.

Application of this approach to the reactions of radical addition to the multiple bonds of the type

$$X^{\bullet} + Y{=}Z \rightarrow X{-}Y{-}Z^{\bullet},$$

(here, the interrelation between E and ΔH is also correctly described by the IP model[8–17]) gives, in the general case, an underestimated r_e value, which is several times smaller than that calculated by quantum chemistry methods. The reason for this inconsistency is that the potential barriers in the transition state are rather flattened. As a result, the imaginary vibrational frequencies appear to be much lower in absolute value than the stretching vibration frequencies $\nu_{Y=Z}$ and ν_{X-Y} for the reactions considered below. Application of the IP model to the addition reactions is illustrated in Fig. 1. In this case, a strong nonlinearity of the transient structures causes the X—Y—Z angles to approach the right angle and curves *2* and *3*, which describe the potential binding energies X—Y and Y—Z, to lie in different planes. These curves can be projected[1] (curves *2′* and *3′*) on an approximate reaction coordinate tangent to the exact reaction coordinate in the transition state. This coordinate describes atomic vibrations at imaginary frequency in the transition state. The intersection point of curves *2′* and *3′* (they can quite correctly be represented by parabolas) to a good accuracy coincides with the transition-state energy. However, the corresponding X—Y and Y—Z bond elongations in the transition state are determined with a large relative error. Here, the absolute error for the slightly varied distance r_{Y-Z} is small, but the error for the distance r_{X-Y} in the transition state appears to be large.

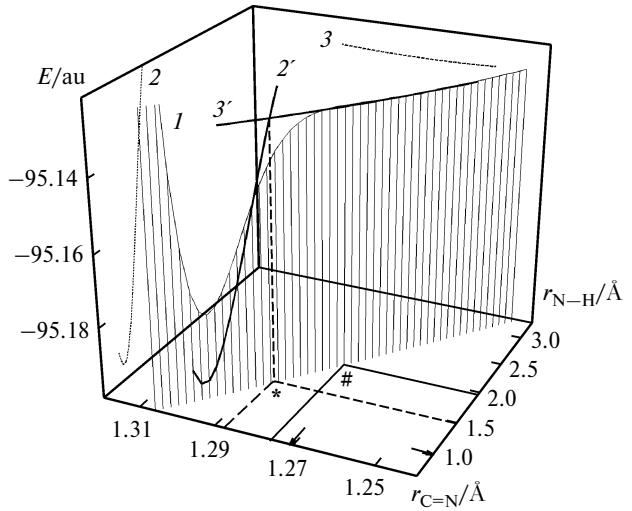

Fig. 1. Potential energy surface of the reaction $H^{\bullet} + HN{=}CH_2 \rightarrow {}^{\bullet}CH_2NH_2$: cross section of the potential energy surface along the approximate reaction coordinate corresponding to the vibration with imaginary frequency in the transition state$^{\#}$, projected on the plane of the C—N and N—H distances (*1*); potential curve describing stretch of the N—H bond in ${}^{\bullet}CH_2NH_2$ radical (*2*); and the potential curve describing stretch of the C—N bond in $NH{=}CH_2$ molecule (*3*); the energy of hydrogen atom was included as a constant. Curves *2′* and *3′* represent the curves *2* and *3* projected on the plane in which the approximate reaction coordinate lies. The intersection point of curves *2′* and *3′* is asterisked. The equilibrium C=N and N—H bond lengths in reagents and products, respectively, are arrowed.

The situation can be improved by introducing[18] a reduced parabola with a much smaller force constant in order to describe the X—Y bond elongation (Fig. 2). The method of estimation of the new force constant value is based on the known correlation between the energies and force constants of the multiple bonds. It is assumed that the reduced force constant value corresponds to the X—Y bond energy, which equals the classical barrier to the reverse reaction, $E_e - \Delta H_e$.

In this study we determined the geometric parameters of transition states of the following radical addition reactions with different structures of the reaction center:

$$H^{\bullet} + CH_2{=}CH_2 \rightarrow {}^{\bullet}CH_2Me, \qquad (I)$$

$$^{\bullet}CH_3 + CH_2{=}CH_2 \rightarrow {}^{\bullet}CH_2CH_2Me, \qquad (II)$$

$$^{\bullet}NH_2 + CH_2{=}CH_2 \rightarrow {}^{\bullet}CH_2CH_2NH_2, \qquad (III)$$

$$^{\bullet}OMe + CH_2{=}CH_2 \rightarrow {}^{\bullet}CH_2CH_2OMe, \qquad (IV)$$

$$H^{\bullet} + CH{\equiv}CH \rightarrow {}^{\bullet}CH{=}CH_2, \qquad (V)$$

$$^{\bullet}CH_3 + CH{\equiv}CH \rightarrow {}^{\bullet}CH{=}CHMe, \qquad (VI)$$

$$H^{\bullet} + N{\equiv}CMe \rightarrow HN{=}C^{\bullet}Me, \qquad (VII)$$

$$H^{\bullet} + HN{=}CH_2 \rightarrow {}^{\bullet}CH_2NH_2, \qquad (VIII)$$

$$H^{\bullet} + H_2C{=}O \rightarrow {}^{\bullet}CH_2OH, \qquad (IX)$$

$$^{\bullet}CH_3 + Me_2C{=}O \rightarrow Bu^tO^{\bullet}. \qquad (X)$$

Calculations were carried out by the density functional method (DFT) and using the model of reduced intersecting parabolas (RIP) and the intersecting parabola and reduced Morse curve (IPRMC) model.

The results of DFT calculations of the X—Y and Y—Z bond elongations in the transition states of reactions (I)—(X) are compared with the results of calculations using the IP,[7] RIP, and IPRMC models.

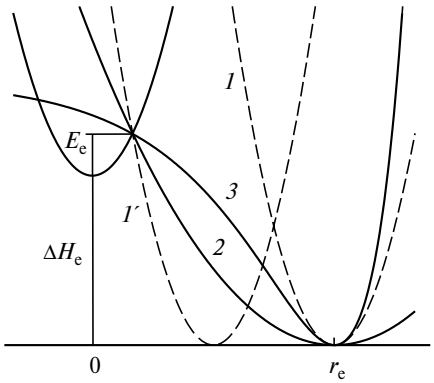

Fig. 2. Potential energy plotted *vs.* interatomic distance for different models of addition reactions: parabola describing the X—Y bond (*1*), shifted parabola passing through the transition state (*1′*), reduced parabola (*2*), and reduced Morse curve (*3*).

Calculation Procedures and Results

Quantum chemical calculations. Hybrid DFT (B3LYP) calculations were carried out using the GAUSSIAN-98 program.[19] Geometric parameters of the structures corresponding to the stationary points on the potential energy surfaces of the systems under study were obtained by optimization in the 6-31G* basis set and then used for energy calculations in the 6-311++G(d,p) basis set with inclusion of zero-point vibrational energy correction calculated in the B3LYP/6-31G* approximation. This approach provides a reasonable accuracy of calculations of the energy barriers to reactions of radical addition to the multiple bonds.[20,21] This also holds for the transition-state geometry of the reactions studied (see below), except for reactions (I), (V), and (VIII) characterized by very early transition states ($r_{H-Y} \approx 2$ Å). In these cases, the transition-state structures are "sensitive" to augmentation of the basis set with the diffuse and polarization functions and to a more correct allowance for correlation effects (our B3LYP/6-31G* calculations gave for r_{H-C} in the transition state of reaction (I) a value of 2.331 Å; *cf.* 1.967 Å according to CCSD(T)/6-311G** calculations[22]). The results of calculations of reactions (I)—(X) are listed in Table 1. The transition-state structures are shown in Fig. 3. Comparison with the results of more accurate calculations[22,23] shows that the X...Y distances in the transition states coincide with an accuracy of 0.1 Å except the corresponding parameters of reactions (I), (V), and (VII)—(IX).

Table 1. Bond lengths (*d*), bond angles (ω), and energies (*E*) of the reagents and transition states (TS), obtained from quantum chemical calculations

System	Geometric parameter				*E*/hartree		
	Bond[a]	$d \cdot 10^{10}$/m	Angle	ω/deg	B3LYP/6-31G*	ZPVE[b]	B3LYP/6-311++G**
H					−0.50027		−0.50226
CH_2CH_2	C—C	1.330			−78.58746	0.05123	−78.61547
$^{\cdot}CH_2Me$	C—C	1.490	H—C—C	112.1	−79.15787	0.05965	−79.18503
	C—H*	1.105					
$H^{\cdot} + CH_2CH_2$	C—H	2.331	H—C—C	104.2	−79.08804	0.05217	−79.11719
TS	C—C	1.337					
$Me^{\cdot}$	C—H	1.083			−39.83829	0.02981	−39.85517
$^{\cdot}CH_2CH_2Me$	C_m—C	1.536			−118.47137	0.08874	−118.50928
	C—C	1.492					
$Me^{\cdot} + CH_2CH_2$	C—C_m	2.263	C—C—C_m	109.9	−118.41878	0.08469	−118.46116
TS	C—C	1.356					
$^{\cdot}NH_2$	N—H	1.034	H—N—H	102.1	−55.87262	0.01898	−55.90038
$^{\cdot}CH_2CH_2NH_2$	N—C	1.470	N—C—C	110.8	−134.49716	0.07815	−134.54933
	C—C	1.489					
$^{\cdot}NH_2 + CH_2CH_2$	N—C	2.235	N—C—C	103.1	−134.46079	0.07466	−134.51422
TS	C—C	1.355					
$MeO^{\cdot}$	C—O	1.369			−115.05046	0.03738	−115.09221
	C—H	1.103					
$^{\cdot}CH_2CH_2OMe$	C—C	1.491	C—O—C	113.1	−193.66938	0.09382	−193.73231
	C—O	1.420	C—C—O	110.6			
	C_m—O	1.414					
$MeO^{\cdot} + CH_2CH_2$	C—C	1.361	C—O—C	112.6	−193.63489	0.09157	−193.70180
TS	C—O	2.067	C—C—O	102.9			
	C_m—O	1.390					

(*to be continued*)

Table 1 (*continued*)

System	Geometric parameter				*E*/hartree		
	Bond[a]	$d \cdot 10^{10}$/m	Angle	ω/deg	B3LYP/6-31G*	ZPVE[b]	B3LYP/6-311++G**
HC≡CH	C—C	1.205			−77.32565	0.02660	−77.35657
$^{\bullet}CH=CH_2$	C—C	1.310	H—C—C	122.2	−77.90121	0.03674	−77.9284
	C—H*	1.096	H—C—C	107.0	−77.82447	0.02760	−77.85611
$H^{\bullet}$ + HC≡CH	C—C	1.213					
TS	C—H	2.076					
$^{\bullet}CH=CHMe$	C_m—C	1.509	C_m—C—C	125.9	−117.22038	0.06606	−117.25843
	C—C	1.313					
$Me^{\bullet}$ + HC≡CH	C_m—C	2.358	C_m—C—C	115.5	−117.15551	0.05949	−117.19986
TS	C—C	1.223					
$CH_2=O$	C—O	1.207			−114.50047	0.02682	−114.54174
$^{\bullet}CH_2OH$	C—O	1.370			−115.05203	0.03752	−115.10230
	O—H	0.969					
$H^{\bullet}$ + $O=CH_2$	O—H	1.568	H—O—C	121.2	−114.99200	0.02779	−115.03573
TS	C—O	1.236					
$Me_2C=O$	C—O	1.216			−193.15569	0.08407	−193.21818
	C—C	1.521					
$Me_3C—O^{\bullet}$	C—O	1.382			−233.00617	0.12310	−233.07878
	C—C	1.541					
$Me^{\bullet}$ + $Me_2C=O$	C—C	2.158	C—C—O	92.5	−232.94989	0.11931	−233.05414
	C—O	1.251					
TS	C—C	1.534					
$HN=CH_2$	C—N	1.271			−94.62721	0.04005	−94.66244
	N—H	1.027					
$^{\bullet}CH_2NH_2$	C—N	1.402			−95.19561	0.05052	−95.23741
	N—H	1.015					
$H^{\bullet}$ + $HN=CH_2$	N—H	1.960	H—N—C	122.3	−95.12774	0.04129	−95.16440
TS	N—H	1.025					
	C—N	1.275					
MeCN	C—N	1.160			−132.75493	0.04564	−132.79604
	C—C	1.461					
$^{\bullet}NHCMe$	C—N	1.244	H—N—C	116.5	−133.29207	0.05539	−133.33858
	C—C	1.493					
	N—H	1.025					
H + NCMe	N—H	1.589	H—N—C	118.6	−133.24736	0.04649	−133.29122
TS	C—N	1.175					
	C—C	1.460					

[a] For nonequivalent bonds, the C atom of the methyl group adding is labeled "m" and the adding H atom is asterisled.
[b] ZPVE is the zero-point vibrational energy correction.

The activation energies and the enthalpies of reactions obtained from DFT calculations and the experimental data are listed in Table 2.

The average errors in determination of the E and ΔH values (12.1 and 17.8 kJ mol^{-1}, respectively) lie within the accuracy limits in the description of energy characteristics by the B3LYP method. Because of high exothermicity of the addition reactions, their transition states usually appear to be very early, being characterized by long $r_{X—Y}$ distances (see Fig. 3). The length of the bond forming in the transition state correlates with the elongation of the multiple bond, namely, the larger the relative bond elongation, the closer the transition-state geometry to the geometry of the initial molecule. However, generally the reactions studied do not obey the rule, according to which the more early the transition state, the lower the activation energy.

Model of intersecting parabolas (IP model).[8—11] The model treats the transition state of an addition reaction as the intersection point of two parabolas, which describe the elongation of the Y=Z multiple bond and the forming X—Y bond in the "bond elongation Δr—potential energy of bond U" coordinates. Each bond is characterized by the coefficient b (force constant is $2b^2$). The reaction is characterized by the following parameters:

1) classical enthalpy ΔH_e, which includes the zero-point vibrational energy difference between the

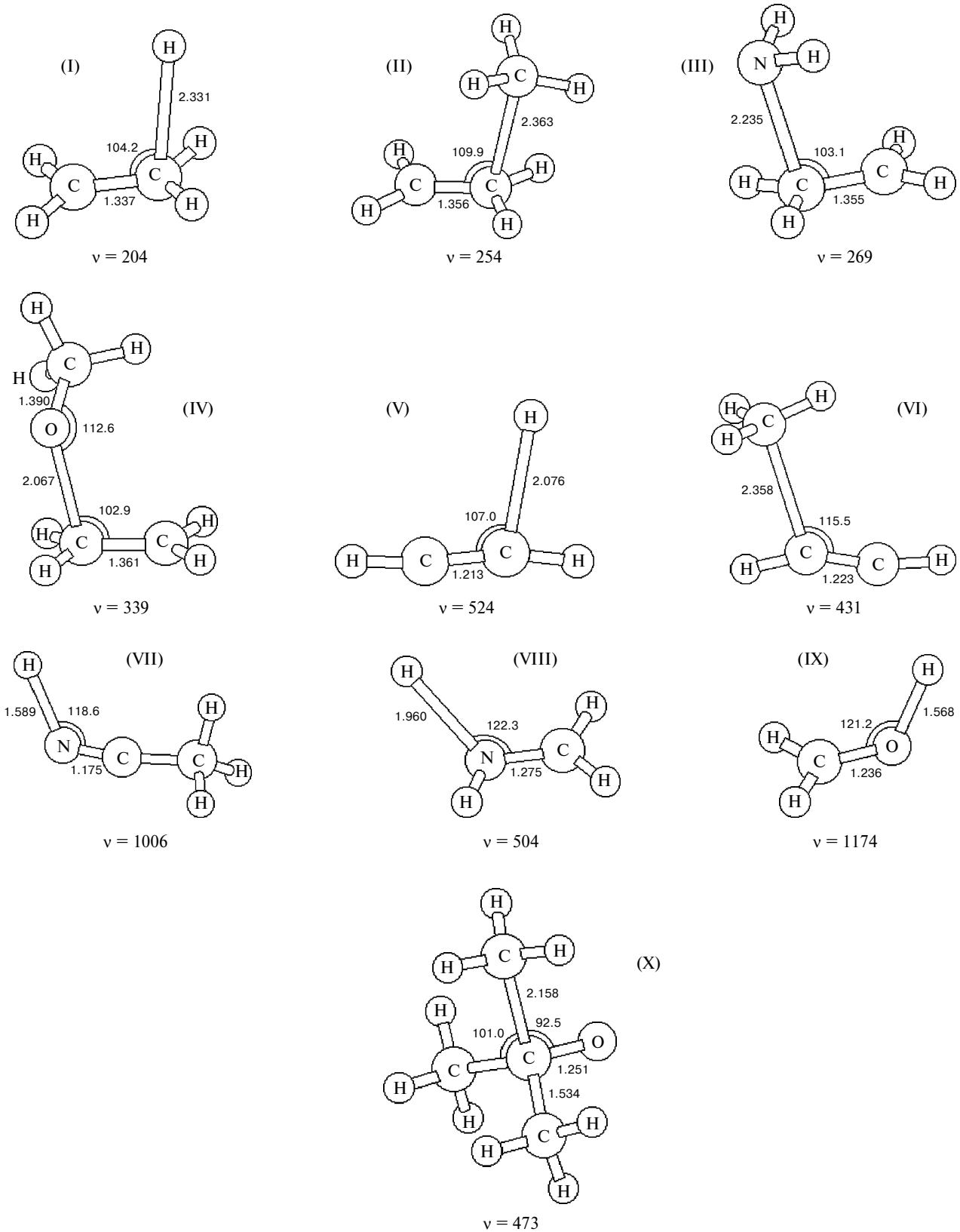

Fig. 3. Transition-state structures of reactions (I)—(X); shown are the bond lengths (in Å) and bond angles (in degrees), and the imaginary vibrational frequencies of the forming bond (in cm^{-1}).

Table 2. B3LYP/6-31G*//B3LYP/6-311++G** calculated activation energies (E/kJ mol^{-1}) and enthalpies (ΔH/kJ mol^{-1}) of addition reactions and experimental data[12–17]

Reaction	E		ΔH	
	Calculations	Experiment	Calculations	Experiment
(I)	3.8	9.9	−154.8	−149.9
(II)	34.3	29.2	−81.2	−101.3
(III)	15.9	16.6	−67.1	−83.0
(IV)	23.2	11.2	−51.0	−77.3
(V)	9.8	18.5	−157.4	−144.7
(VI)	39.2	16.5	−97.3	−108.9
(VII)	20.8	28.1	−80.2	−50.5
(VIII)	4.2	24.0	−167.4	−145.1
(IX)	24.3	23.7	−125.1	−110.2
(X)	63.0	31.3	+10.0	−25.1

broken bond (Y=Z) and the newly forming bonds (X—Y and Y—Z)

$$\Delta H_e = \Delta H_e + 0.5hL(\nu_{Y=Z} - \nu_{Y-Z} - \nu_{X-Y}), \quad (3)$$

2) classical height, E_e, of potential barrier, which differs from the experimentally measured activation energy, E, by the kinetic energy necessary to bring reagents close together during the motion along the reaction coordinate*

$$E_e = E - 0.5RT, \quad (4)$$

3) coefficient b relating the vibrational frequency to the vibrational energy of the multiple bond (this parameter depends on the vibrational frequency ν and the reduced mass, μ, of the atoms involved in a given bond):

$$b = 2\pi\nu_{Y=Z}\mu^{0.5}, \quad (5)$$

4) coefficient $\alpha = b/b_f$, where b_f characterizes the forming bond X—Y, and

5) total elongation, r_e, of the reacting bonds.

The parameters of the model are interrelated as follows

$$br_e = \alpha\sqrt{E_e - \Delta H_e} + \sqrt{E_e}. \quad (6)$$

The elongation of the attacked bond and the elongation of the newly forming bond in the transition state are given by

$$r^{\#} = \sqrt{E_e}/b \quad (7)$$

and

$$r_e - r^{\#} = \sqrt{E_e - \Delta H_e}/b_f. \quad (8)$$

respectively.

* Since addition reactions are usually characterized by early transition states, the Y=Z vibrational frequency difference between the reagent and transition state is small and can be ignored.

Reduced intersecting parabolas (RIP) model.[18] This model treats the activation energy for a reaction as the intersection point of the parabola characterizing the elongation of the multiple bond Y=Z with the parabola characterizing the elongation of the X...Y bond with a reduced value of the parameter $b_f^{\#}$. The $b_f^{\#}$ value is determined from an empirical equation[18]

$$b_f^{\#} = aD_{ef}^{\#} - cD_{ef}^{\#2}, \quad (9)$$

where the reduced bond energy is $D_{ef}^{\#} = E_e - \Delta H_e$. The method for calculating empirical coefficients a and c and their values were reported earlier.[18] The parameter r_e is calculated as follows:

$$r_e = \sqrt{E_e}/b + \sqrt{E_e - \Delta H_e}/b_f^{\#}. \quad (10)$$

When no experimental data for E are available, the classical barrier height E_e is calculated using the IP model *via* ΔH_e [8]

$$\sqrt{E_e} = \frac{br_e}{\alpha^2 - 1}\left[\alpha\sqrt{1 + \frac{\alpha^2 - 1}{(br_e)^2}\Delta H_e} - 1\right] \quad (11)$$

and the known br_e value. The interatomic distances, zero-point vibrational energies, and the parameters b and b_f for the bonds in the molecules under study are listed in Table 3.

The enthalpies of reactions were calculated from the thermochemical equations:

$$\Delta H = \Delta H_{XYZ}\cdot - \Delta H_{Y=Z} - \Delta H_{X}\cdot, \quad (12)$$

$$\Delta H_{X}\cdot = \Delta H_{XH} + D_{X-H} - \Delta H_{H}\cdot. \quad (13)$$

Calculations were carried out using the published bond dissociation energies D_{X-H},[10,25] and enthalpies of forma-

Table 3. Parameters of the chemical bonds involved in reactions (I)—(X): bond length (r), coefficient b, and zero-point vibrational energy correction ($0.5hL\nu$)[11,24]

Bond	$r\cdot10^{10}$ /m	$b\cdot10^{-10}$ /kJ$^{0.5}$ mol$^{-0.5}$ m^{-1}	$0.5hL\nu$ /kJ mol^{-1}
>C—H	1.092	37.43	17.4
C=CH—H	1.077	39.61	18.4
RO—H	0.967	47.01	21.7
RNH—H	1.009	43.06	20.0
C—CH_3	1.513	44.83	8.2
C—NH_2	1.469	38.22	6.8
C—OR	1.416	38.14	6.6
C=C	1.299	53.89	9.9
C≡C	1.183	69.12	12.7
C=O	1.210	59.91	10.3
C=N	1.271	56.50	10.0
C≡N	1.136	59.91	13.5

Table 4. Enthalpies (ΔH_e), kinetic parameters (α, br_e), and activation energies (E_e) for addition reactions (I)—(X)[11—17]

Reaction	α	$-\Delta H_e$	E_e	br_e
		kJ mol^{-1}		/kJ$^{0.5}$ mol$^{-0.5}$
(I)	1.440	166.1	8.7	21.99
(II)	1.202	106.7	28.0	19.24
(III)	1.410	88.1	15.4	18.27
(IV)	1.413	82.2	10.1	16.75
(V)	1.847	160.3	17.3	28.77
(VI)	1.542	114.3	15.3	21.47
(VII)	1.768	67.0	26.9	22.32
(VIII)	1.312	161.9	22.8	22.61
(IX)	1.600	128.2	22.4	24.37
(X)	1.336	29.6	30.1	15.81

tion of the molecules.[26,27] The parameters α, br_e, ΔH_e, and the E_e values calculated for the reactions under study using Eqn. (11) are listed in Table 4. The error in estimation of the parameter r_e is determined by the error in determination of the parameters ΔH and E for a given reaction and varies within the range $(6—9)\cdot 10^{-13}$ m.[11—14] This is comparable with the error in bond length measurements by physical methods ($(5—10)\cdot 10^{-13}$ m).

Intersecting parabola and reduced Morse curve (IPRMC) model. An alternative method of correction of the IP model is to describe the X—Y bond elongation by a reduced Morse curve. Clearly, the Morse curve describing cleavage of the X—Y bond in the X—Y—Z$^{\bullet}$ radical at the dissociation limit equal to $-\Delta H_e$ can not be used for calculation of the energy barrier to a reaction. Besides, the case for positive ΔH_e values can not be described in this approach at all. Therefore, we assume that the dissociation limit equals the vertical dissociation energy of the X—Y bond in the X—Y—Z$^{\bullet}$ radical, which corresponds to a constant distance $r_{Y—Z}$. The modified dissociation limit value qualitatively corresponds to the definition of $D_{ef}^{\#}$ in the RIP model and provides the best description of the potential energy in the vicinity of the transition state.

The model treats the transition state of a radical addition reaction as the intersection points of a parabola and a reduced Morse curve. The parabola describes the variation of the potential energy caused by the elongation of the multiple bond Y=Z and depends on the coefficient b only (see expression (5)). The reduced Morse curve characterizes variation of the potential energy on stretching the X—Y bond in the addition product X—Y—Z$^{\bullet}$ ignoring relaxation of the Y—Z bond length. The shape of this curve is governed by the coefficient b_f ($b_f = 2\pi\nu_{XY}\sqrt{\mu_{XY}}$) and by the vertical bond dissociation energy, which can be determined as follows

$$D_{ef}^{*} = -\Delta H_e + [0.8 b_{Y=Z}(r_{Y—Z} - r_{Y=Z})]^2. \qquad (14)$$

The numerical coefficient 0.8 in expression (14) appears as a result of shortening of the Y—Z bond in the radical compared to its value in the saturated molecules. According to calculations, the relative elongations of the multiple bonds C=C, C≡C, C=O, and C≡N upon H$^{\bullet}$ addition are similar (80, 85, 75, and 76% of the total elongation of the multiple bond, respectively). The C=N bond elongation upon H$^{\bullet}$ addition to methyleneimine is somewhat smaller (68%). Therefore, the average value of coefficient was taken to be 0.8. The other reaction parameters are the same as those used in the IP model (see above). The elongation of the multiple bond Y=Z in the transition state ($r^{\#}$) is calculated using expression (7) and the elongation of the forming bond X—Y ($\Delta r_{X—Y}$) and the total elongation of the bonds in the transition state (r_e) are found from the relationships

$$\Delta r_{X—Y} = \frac{\sqrt{D_{ef}^{*}}}{b_f} \ln \frac{\sqrt{D_{ef}^{*}}}{\sqrt{D_{ef}^{*}} - \sqrt{E_e - \Delta H_e}} \qquad (15)$$

and

$$r_e = r^{\#} + \Delta r_{X—Y}, \qquad (16)$$

respectively.

Comparison of the results of calculations of the $\Delta r_{Y—Z}$ and $\Delta r_{X—Y}$ values. The $r^{\#}$ and $\Delta r_{X—Y}$ values calculated from experimental data (enthalpies and activation energies) are listed in Table 5. The B3LYP calculated bond lengths are somewhat different from the experimental values (*cf.* the data in Tables 1 and 3). Keeping in mind a possible compensation of errors, DFT calculations of bond elongations (Table 5) were carried out using the reference bond length values for the reagents (see Table 3). According to quantum chemical calculations, elongation of the

Table 5. Elongations of interatomic distances in transition states ($r^{\#}$) and $\Delta r_{Y...X}$ for addition reactions calculated by different methods

Reaction	$r^{\#}\cdot 10^{10}$/m		$\Delta r_{Y...X}\cdot 10^{10}$/m			
	I	II	I	II	III	IV
(I)	0.055	0.007	0.353	1.226	0.708	0.761
(II)	0.098	0.026	0.259	0.727	0.656	0.562
(III)	0.073	0.025	0.266	0.765	0.727	0.510
(IV)	0.074	0.031	0.252	0.647	0.527	0.460
(V)	0.060	0.008	0.356	0.980	0.704	1.001
(VI)	0.057	0.018	0.392	0.849	0.594	0.679
(VII)	0.087	0.015	0.398	0.564	0.797	0.640
(VIII)	0.084	0.004	0.316	0.945	0.603	0.747
(IX)	0.079	0.020	0.407	0.599	0.494	0.542
(X)	0.092	0.035	0.230	0.617	0.826	0.291

Note: I — IP model, II — DFT calculations, III — RIP model, and IV — IPRMC model.

multiple bond in the transition state is small (3—7% of the total bond elongation, or 0.004—0.03 Å). The smallest elongation of the multiple bond (0.004 Å) was found for reaction (VIII). It is due to a marked shortening of the C—N bond in the forming radical compared to the corresponding bond length in the $MeNH_2$ molecule. The IP, RIP, and IPRMC methods give larger multiple bond elongations (0.06 to 0.1 Å). As mentioned above, the IP model strongly underestimates the bond elongation value. The RIP calculated distances Δr_{X-Y} best approach the results of DFT quantum chemical calculations for all reactions, except the $H^{\bullet}$ addition reactions. The largest differences between the results of calculations using the RIP and IPRMC models and the results of DFT calculations were found for reaction $H^{\bullet} + C_2H_4$. On the other hand, these data are in reasonable agreement with the results of more accurate calculations[22] ($\Delta r_{H-C} = 0.875$ Å). This shows that the method developed in this work permits estimation of true elongations of the key bonds in transition states of radical reactions. Thus, out of the three semiempirical models of addition reactions it is the RIP model that in most cases provides the best agreement between the semiempirically calculated transition-state geometries and the results of DFT quantum chemical calculations.

Comparison of the results of semiempirical (RIP model) and DFT quantum chemical calculations of transition-state geometries carried out in this study allows elaboration of a rather simple semiempirical algorithm of calculations of the interatomic distances in transition states of addition reactions from experimental data. To obtain the same elongations of the interatomic distances in transition states as those found from DFT calculations using only the enthalpy of reaction, it is necessary to introduce two correction parameters, namely, $\beta = r_e(\text{DFT})/r_e(\text{RIP})$ and $b_m = E_e^{1/2}/r^{\#}$ (DFT). The values of these parameters and the parameters a and c (see expression (9)) are listed in Table 6.

Table 6. Empirical parameters (a, b_m, c, β) used in calculations of transition-state geometries from experimental data[17]

Reaction	$b_m \cdot 10^{-10}$ /kJ$^{0.5}$ mol$^{-0.5}$ m^{-1}	β	$a \cdot 10^{-8}$ *	$c \cdot 10^{-6}$ **
(I)	421.4	1.732	12.12	0.82
(II)	203.5	1.143	16.40	1.24
(III)	157.0	1.052	14.80	1.24
(IV)	102.5	1.227	22.80	3.32
(V)	520.0	1.392	12.12	0.82
(VI)	217.3	1.429	16.40	1.24
(VII)	345.8	0.708	13.71	0.82
(VIII)	1194	1.567	13.71	0.82
(IX)	236.6	1.212	19.50	1.99
(X)	156.7	0.747	16.40	1.24

* In kJ$^{-0.5}$ mol$^{0.5}$ m^{-1}.
** In kJ$^{-1.5}$ mol$^{1.5}$ m^{-1}.

The $r_{Y...X}$ and $r_{Y...Z}$ distances in transition states are calculated as follows. First, the enthalpy ΔH and ΔH_e are calculated from thermochemical data for a given reaction (see expression (1)). Next, the E_e value is calculated from experimental data or using expression (11). The coefficient $b_f^{\#}$ is found from Eqn. (9) using the E_e and ΔH_e values. The distance $r_{Y...Z} = r_{Y=Z} + r^{\#}$ is calculated by the expression

$$r_{Y...Z} = r_{Y=X} + \sqrt{E_e}/b_m, \qquad (17)$$

where b_m is the reduced coefficient b, which provides coincidence of the interatomic distances obtained by the RIP and DFT methods for a given class of reactions. The distance $r_{Y...X}$ in transition state is calculated using the expression

$$r_{X...Y} = r_{X-Y} + \frac{\beta\sqrt{E_e - \Delta H_e}}{a(E_e - \Delta H_e) - c(E_e - \Delta H_e)^2}. \qquad (18)$$

Because of the use of experimental distances r_{Y-X} and $r_{Y=Z}$ in expressions (17) and (18), the transition-state geometric parameters are somewhat different from those obtained from B3LYP/6-31G* calculations. However, owing to compensation of errors (see above), it is possible that these values will appear to be close to true values.

Thus, based on comparison of the interatomic distances obtained from the DFT and the RIP model calculations, we have elaborated a simple semiempirical algorithm for calculating transition-state geometries of the reactions of radical addition to the multiple bond from the enthalpies of and activation energies for the reactions. This makes it possible to systematically investigate the transition-state geometries of various radical addition reactions and to analyze the factors determining them.

This work was financially supported by the Chemistry and Materials Science Division of the Russian Academy of Sciences (in the framework of the Program No. 1 "Theoretical and experimental investigations on the nature of chemical bonding and mechanisms of the most important chemical reactions and processes").

References

1. A. F. Shestakov and E. T. Denisov, *Izv. Akad. Nauk*, *Ser. Khim.*, 2003, 307 [*Russ. Chem. Bull., Int. Ed.*, 2003, **52**, 320].
2. T. G. Denisova, E. T. Denisov, A. F. Shestakov, and N. S. Emel´yanova, *Khim. Fiz.*, 2003, **22**, 29 [*Chem. Phys. Reports*, 2003, **22** (Engl. Transl.)].
3. T. G. Denisova, E. T. Denisov, A. F. Shestakov, and N. S. Emel´yanova, *Izv. Akad. Nauk*, *Ser. Khim.*, 2004, 693 [*Russ. Chem. Bull., Int. Ed.*, 2004, **53**, 727].
4. T. G. Denisova and E. T. Denisov, *Kinet. Katal.*, 2004, **45**, 1 [*Kinet. Catal.*, 2004, **45**, 1 (Engl. Transl.)].

5. T. G. Denisova and N. S. Emel´yanova, *Kinet. Katal.*, 2003, **44**, 485 [*Kinet. Catal.*, 2003, **44**, 441 (Engl. Transl.)].
6. T. G. Denisova and E. T. Denisov, *Kinet. Katal.*, 2004, **45**, 877 [*Kinet. Catal.*, 2004, **45**, 826 (Engl. Transl.)].
7. A. F. Shestakov, *Dokl. Akad. Nauk*, 2003, **393**, 611 [*Dokl. Phys. Chem.*, 2003, **393**, 339 (Engl. Transl.)].
8. E. T. Denisov, *Kinet. Katal.*, 1992, **33**, 66 [*Kinet. Catal.*, 1992, **33**, 50 (Engl. Transl.)].
9. E. T. Denisov, in *General Aspects of the Chemistry of Radicals*, Ed. Z. B. Alfassi, Wiley, New York, 1999, 79.
10. E. T. Denisov, T. G. Denisova, and T. S. Pokidova, in *Handbook of Free Radical Initiators*, Wiley, New York, 2003, 423.
11. E. T. Denisov, *Usp. Khim.*, 2000, **69**, 166 [*Russ. Chem. Rev.*, 2000, **69**, 153 (Engl. Transl.)].
12. E. T. Denisov and T. G. Denisova, *Khim. Fiz.*, 1998, **17**, 83 [*Chem. Phys. Reports*, 1998, **17**, 2105 (Engl. Transl.)].
13. E. T. Denisov, *Izv. Akad. Nauk*, *Ser. Khim.*, 1999, 445 [*Russ. Chem. Bull.*, 1999, **48**, 442 (Engl. Transl.)].
14. E. T. Denisov, *Kinet. Katal.*, 1999, **40**, 835, [*Kinet. Catal.*, 1999, **40**, 56 (Engl. Transl.)].
15. E. T. Denisov, *Kinet. Katal.*, 2000, **41**, 325 [*Kinet. Catal.*, 2000, **41**, 293 (Engl. Transl.)].
16. E. T. Denisov, *Kinet. Katal.*, 2001, **42**, 30 [*Kinet. Catal.*, 2001, **42**, 23 (Engl. Transl.)].
17. E. T. Denisov, *Khim. Fiz.*, 2003, **22**, Iss. 9, 40 [*Chem. Phys. Reports*, 2003, **22**, Iss. 9 (Engl. Transl.)].
18. E. T Denisov, *Izv. Akad. Nauk*, *Ser. Khim.*, 2004, 1542 [*Russ. Chem. Bull., Int. Ed.*, 2004, **53**, 1602].
19. M. J. Frisch, G. W. Trucks, M. Head-Gordon, P. M. W. Gill, M. W. Wong, J. B. Foresman, B. G. Johnson, H. B. Schlegel, M. A. Robb, E. S. Replogle, R. Gomperts, J. L. Anders, K. Raghavachari, J. S. Binkley, C. Gonzales, R. L. Martin, D. J. Fox, D. J. Defrees, J. Baker, J. J. P. Stewart, and J. A. Pople, *GAUSSIAN-98, Revision A6*, Gaussian Inc., Pittsburgh (PA), 1998.
20. H. Hipper and B. Vuskolcz, *Phys. Chem. Chem. Phys.*, 2002, **4**, 4663.
21. S. L. Boyd and R. J. Boyd, *J. Chem. Phys.*, 2001, **105**, 7096.
22. J. Villa, A. Gonzales-Lafont, J. M. Lluch, and D. G. Truhlar, *J. Am. Chem. Soc.*, 1998, **120**, 5599.
23. V. Barone and L. Orlandi, *Chem. Phys. Lett.*, 1995, **245**, 45.
24. D. R. Lide, *Handbook of Chemistry and Physics*, CRC Press, Boca Raton, 1992.
25. Y.-R. Luo, *Handbook of Bond Dissociation Energies in Organic Compounds*, CRC Press, Boca Raton, 2003.
26. *NIST Standard Reference Database 19A. Positive Ion Energetics, Version 2.02*, Gaithersburg, 1994.
27. E. T. Denisov and S. L. Khursan, *Russ. J. Phys. Chem.*, 2000, **74**, Suppl. 3, 491.

Received February 10, 2004